Pathogenic bacteria grown in iron and zinc milieu exhibit magnetotaxis

Pathogenic bacteria make magnetic nanoparticles

Summary Pathogenic bacteria treated with iron and zinc precursors form intracellular magnetic nanoparticles and display magnet-induced migration.

Swati Kaushik[1], Jijo Thomas[1], Vineeta Panwar[1], Preethi M[1], Rupali Singh[1], Himadri Shekar Roy[1], Rajesh Kumar[2], Vianni Chopra[1], Vikas Gautam[2], Deepa Ghosh[1*]

[1] Chemical Biology Unit, Institute of Nano Science and Technology, Knowledge City, Sector 81, Mohali, Punjab 140306, India

[2] Post Graduate Institute of Medical Education & Research (PGIMER), Chandigarh, India

Abstract

Magnetotactic bacteria (MTB) are the only microorganisms that are known to form intracellular magnetic nanoparticles. Iron and zinc are important elements required for the survival of pathogenic bacteria. While the host immunity prevents the bacteria easy access to these elements, virulent bacteria have evolved multiple mechanisms to access these elements. The response of pathogenic bacteria like *Staphylococcus aureus*, *Escherichia coli*, *Pseudomonas aeruginosa* and *Klebsiella pneumoniae* was evaluated in the presence of iron and zinc. The treated bacteria revealed intracellular distribution of superparamagnetic nanoparticles comprising of zinc ferrite, and the bacteria responded to magnetic field with magnetotaxis. Similar intracellular biomineralization was observed in bacteria obtained from blood specimens of patients with sepsis. In brief, this study provides a hitherto unknown phenomenon of bacterial biomineralization.

Magnetotactic bacteria (MTB) are a group of Gram-negative prokaryotes that passively align and effectively swim along the geomagnetic field (*1*). Blakemore described this movement in response

to magnet as "magnetotaxis", which begot the term MTB for such bacteria (*2*). The magnetic nanoparticles in these microorganisms are present in explicit structures termed magnetosomes and the process of biosynthesis is termed bio-mineralization (*3).* These bacteria are fastidious and have an extremely slow rate of biomineralization (>1 week) (*4*). Apart from magnetotactic bacteria, a class of bacteria termed 'iron reducing bacteria' is reported to synthesize magnetic nanoparticles extracellularly in presence of iron precursors (*5, 6*). Magnetic nanoparticle biosynthesis was achieved in a non-magnetotactic bacterium by transferring the entire genetic machinery of magnetosome to a non-magnetotactic, *Rhodospirillum rubrum* (*7*). Apart from this, no other bacteria have been reported to form *in situ* magnetic nanoparticles.

Iron and zinc are transient elements that are essential for virtually all organisms. While these elements are required for the survival of bacteria, the host prevents the invading bacteria from accessing these elements by associating these elements with cellular components or regulating their availability through nutritional immunity (*8*). To facilitate their survival and replication, pathogenic bacteria have evolved multiple strategies to acquire these elements from various host resources (*9*). Whereas several reports have shown the individual effect of either iron or zinc on pathogenic microbes, no report on their combined effect exists (*10*). Given the importance of these transition metals to pathogenic bacteria and the possible intertwining between iron and zinc homeostasis (*11,12*), we evaluated the response of pathogenic bacteria like *Staphylococcus aureu, Escherichia coli, Pseudomonas aeruginosa, and Klebsiella pneumoniae* to a combination of iron and zinc precursors. Of these, *S. aureus* is a Gram-positive bacterium, and the other 3 are Gram-negatives. Each bacterium was cultured in a broth containing a mixture of 1mM $FeCl_2$ and zinc gluconate for 24-48 h. A faint time-dependent darkening of broth was visible in the respective treated cultures (**Fig S1**). Microscopic evaluation of the treated cultures revealed microbial aggregation in the treated bacteria (**Fig 1 B&F, S2**), in comparison to untreated control (**Fig 1 A&E, S2**). On exposure to a magnetic field, only those microbes that were grown in the presence of iron and zinc exhibited magnetotaxis (**Video S3-S10**). To confirm whether the magnetic response is facilitated by intracellular iron, we performed Perls Prussian blue staining. The blue color was observed solely in bacteria treated with Fe and Zn and also indicated the importance of zinc in intracellular iron uptake. (**Fig. 1 C&G, S11**). Fe and Zn content in the respective bacteria was estimated using IC-PMS (**Table S1**) In all the microbes tested, despite differences in the

intracellular content of various strains, an increase in iron content was observed only in those microbes treated with iron and zinc, thus supporting our results obtained with Prussian blue studies (**Fig S11, Table S1).** . To verify if the intracellular zinc, like iron was present in its oxide form, confocal imaging was performed. **Figure 1 D&H** shows faint red fluorescence, indicating zinc oxide presence.

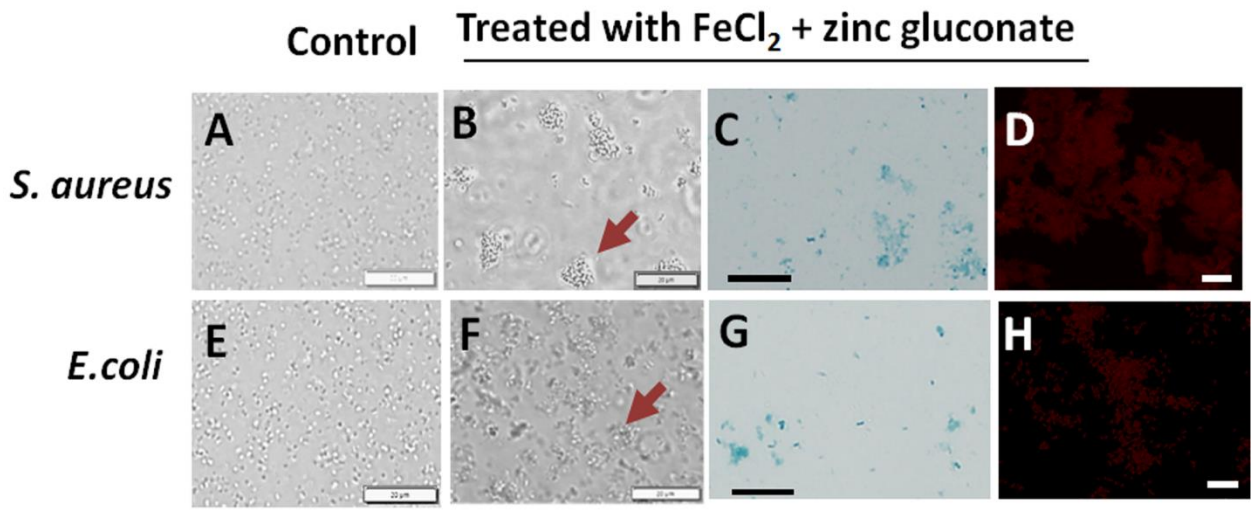

Fig. 1: Bacterial response to Fe and Zn. Upper panel shows *S. aureus,* lower panel *E. coli* respectively. Bright field images of untreated (**A, E**) and treated bacteria, (**B, F**). Arrow shows bacterial aggregates (**C, G**) Treated bacteria stained blue with Perls Prussian blue; (**D, H**) Faint red fluorescence in treated bacteria visualized using confocal microscope. Scale bar represents 20 μM.

The Gram-positive (*S. aureus)* and a representative Gram-negative bacterium (*E.coli)* were taken up for further evaluation. TEM analysis of $FeCl_2$ and Zinc gluconate treated *S. aureus* and *E. coli* revealed the presence of significant number of nanocrystals distributed throughout the respective bacteria (**Fig 2 B, F**) as compared to untreated control (**Fig 2 A, E**), confirming *in situ* biosynthesis. On further analysis of the respective bacterial lysates, Quasi-cuboidal shaped particles (**Fig S12A)** of 13-19 nm size were observed (**Fig S12B)** (*13*). HR-TEM images of individual nanocrystals clearly showed the lattice fringes, indicating the crystalline nature of the material (*14*). The inter-planar spacing calculated from these fringes exhibited d-spacing of 0.283 nm and of 0.489 nm corresponding to 100 planes of ZnO and 111 planes of zinc ferrite ($ZnFe_2O_4$)

respectively **(Fig 1C, G)** (*13, 15*). The diffraction spots indexed from selected area electron diffraction pattern (SAED) confirmed its crystalline nature having (111), (311), (220), (400), (511), (440) planes of ZnFe2O4 and (100), (101), (110) plane of ZnO **(Fig. 2 D, H)** (*16*). EDAX analysis **(Fig S12C)** and elemental mapping **(Fig S13)** confirmed the presence of iron, zinc and oxygen with homogeneous distribution of the above-mentioned elements. To evaluate the magnetic properties of the nanoparticles, field dependent magnetization measurements were performed on treated bacteria after lyophilization using a Superconducting Quantum Interference Device (SQUID). **Fig 2** displays the magnetic properties (M-H loop at 300K (I), at 5K (J) and M-T curve (K)) with *S. aureus*. At room temperature (300K), negligible coercivity was observed indicating the superparamagnetic behavior of the nanoparticles due to zero coercivity (inset, **Fig 2I**). The magnetic signal observed at 5 K displayed low coercivity (150 Oe: inset **Fig 2J**), confirming the characteristic properties of superparamagnetism (*17*) The zero field cooled (ZFC) and field cooled (FC) curves of the samples obtained at an applied field of 500 Oe further confirmed the superparamagnetic behavior with blocking temperature at ~ 150 K (**Fig. 2K**). A similar observation was observed with *E. coli* (**Fig S14).** As the superparamagnetism characteristics are generally exhibited by magnetic nanoparticles that exist as single domain particles, it can be concluded that the magnetic particles present in the treated bacteria are also single-domain superparamagnetic nanoparticles (*18*). Additionally, zinc ferrite nanoparticles are reported to have better magnetization properties than iron oxide nanoparticles, which could be contributing to the observed magnetotaxis (*19*).

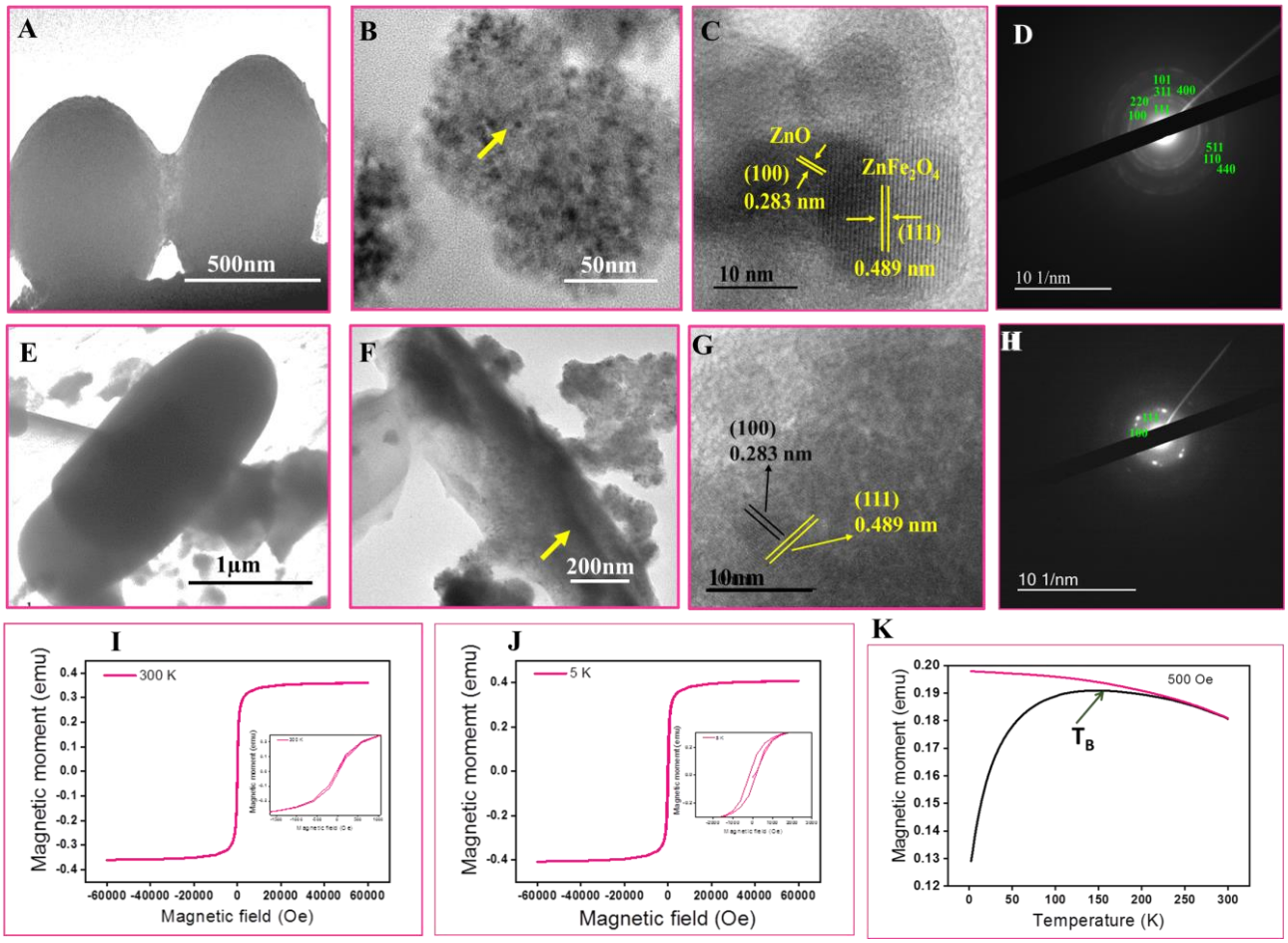

Fig.2 Characterization of nanoparticles. The upper and lower panel shows TEM images of *S. aureus* and *E. coli* respectively. (**A, E**) Untreated bacteria; (**B, F**) Bacteria treated with $FeCl_2$ and zinc gluconate (arrow indicates nanoparticles); (**C, G**) HR-TEM showing D-Planar spacing of nanoparticles; (**D, H**) SAED pattern of nanoparticles; **Magnetic measurement studies of nanoparticles in S. *aureus*.** Treated bacteria were lyophilized and magnetization versus magnetic field was measured at (**I**) 300 K, (**J**) 5K and inset represents coercivity. (**K**) Measurement of Temperature Dependence of Magnetization (FC/ZFC curves).

Further characterization of the treated bacteria using XRD revealed the crystalline nature of *in situ* formed material (**Fig S15A).** The numerous strong Bragg reflections could be indexed to the presence of both ZnO and zinc ferrite phases (*15*) respectively supporting the TEM results. The crystalline peaks at $2\theta = 31.73^{o}$, 36.2^{o} and 56.6^{o} represents (100), (101), (110) hkl plane correspond to the hexagonal crystal structure of ZnO according to JCPDS no. 36-1451 (*20*). The peaks at $2\theta = 18.3^{o}$, 30.1^{o}, 35.2^{o}, 43.1^{o}, 53.3^{o}, 56.7^{o} and 62.4^{o} with hkl plane of (111), (220), (311), (400),

(422), (511) and (440) correspond to the cubic spinel structure of $ZnFe_2O_4$ according to JCPDS no. 79-1150 (*16*). Fourier transform infrared (FTIR) analysis of the treated bacteria post its lyophilization also exhibited peaks in the region from 670-550 cm^{-1} reflecting the stretching vibration mode associated to Fe–O bonds in the crystalline lattice of $ZnFe_2O_4$ (*14*). The other peaks observed in the region from 476-417 cm^{-1} indicated the presence of Zn-O bond (**Fig S15 C, D)** (*14*). The presence of N-H stretch between 3,500-3,100 cm^{-1} in the full scan FTIR spectra could be contributed by the proteins present in the bacterial cells **(Fig S15B).** These results reconfirmed the presence of zinc ferrite and zinc oxide in the treated bacteria.

While the exact mechanism of biosynthesis is unclear, it can be construed that on uptake, soluble Fe (II), in the presence of oxygen would induce oxidative stress via the Fenton reaction. We evaluated the oxidative stress in the respective microbes using ROS assay. As displayed in **Fig S16,** treatment with iron *per se* increased ROS levels in pathogenic bacteria. In comparison, the bacteria treated with zinc alone, and in combination with iron, displayed an additional increase in ROS levels. This data reaffirmed the role of zinc in inducing oxidative stress (*21*). The results suggested that in comparison to iron, zinc was a more potent inducer of ROS. This data is supported by a recent study in which excess zinc was shown to increase both intracellular iron and oxidative stress in *E. coli* (*10*). It is likely that ROS is involved in the biomineralization process, as only those microbes expressing high levels of ROS revealed significant iron accumulation and nanoparticle synthesis. In an earlier study, we reported the role of ROS in inducing iron nanoparticle synthesis in eurkaryotic cells treated with a similar combination of Fe and Zn precursors (*22*). Although ROS expression appears to be common among the two studies, the phenomenon of biomineralization observed in these bacteria is intriguing and throws up several questions that are worth further investigation.

The uptake of iron/zinc in bacteria is regulated by the metal-dependent Fur/Zur family of protein which controls the respective genes involved in their acquisition. Apart from normal physiological processes, these regulatory proteins in pathogenic bacteria are responsible for the expression of virulence factors (*23*) To ensure that intracellular iron/zinc is maintained in its non-toxic form, these bacteria have evolved highly sophisticated systems to balance the efflux/influx of these ions through multiple transport/scavenging/storage systems (*8, 10*). Post-treatment survival of the bacteria on agar plates further confirmed that intracellular iron and zinc accumulation was non-

toxic to the microbes (**Fig S17).** Our results suggested that apart from the previously known pathways of Fe and Zn regulation, the pathogenic bacteria store excess iron/zinc in its oxide form. To confirm this, we tested multiple blood specimens obtained from patients admitted with sepsis at PGIMER hospital, Chandigarh. The pathogenic bacteria in each specimen was identified by Gram-staining (**Fig 3 A, D, S18 A, D, G**) and the respective samples were additionally stained with Perls Prussian blue. A faint blue color, indicated presence of iron oxide (**Fig 3 B, E, S18 B, E, H**). The faint blue color could be attributed to the depletion of oxides of iron, as the bacteria used in these studies were evaluated after a period of 48-72 h post-blood collection. Nevertheless, on exposure of a suspension of carbonized bacterial residue to a magnetic field, aggregation of magnetic particles was visualized (**Fig 3 C, F, S18 C, F, I**). The response of these aggregates to magnetic field, confirmed magnetic nanoparticle synthesis in these bacteria (**Fig S19-S20).**

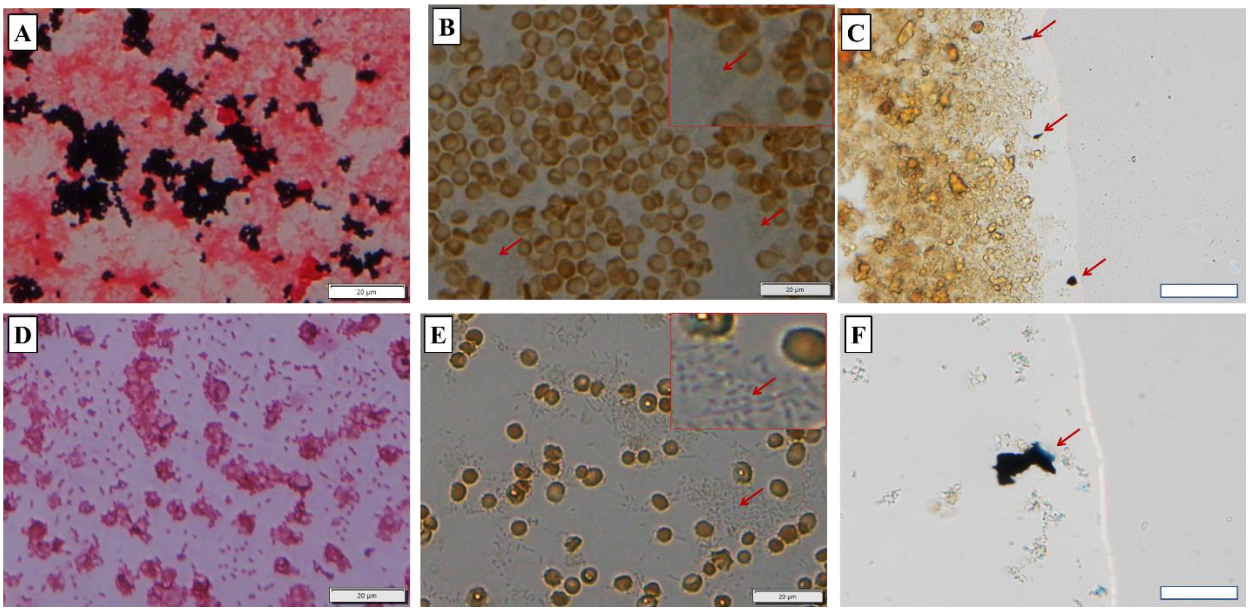

Fig. 3: Clinical specimens tested for iron oxide. Upper panel shows *S. aureus*, lower panel *E. coli* respectively. **(A, D).** Gram-staining of respective bacteria; **(B, E)** Blood smears of respective bacteria were stained with Perls Prussian blue. Arrows show faint blue color staining obtained with Prussian blue, indicating the presence of iron oxide. Inset displays images at higher magnification **(C, F)** Arrows show aggregated magnetic nanoparticles in response to magnetic field. Scale bar represents 20 μM.

The presence of magnetic nanoparticles has been reported in a wide variety of human tissues (*24*).While the reason for its existence remains unexplored, recent reports demonstrating magnetite synthesis in human cells following magnetosome/magnetic nanoparticles exposure (*25, 26*), throws up the possibility of magnetite present in the pathogenic bacteria serving as a trigger for such formation.

References

1. C. T. Lefèvre, D.A. Bazylinsk, Ecology, diversity, and evolution of magnetotactic bacteria. *Microbiol Mol Biol Rev*. **77**(3), 497–526 (2013).
2. R. Blakemore, Magnetotactic bacteria *Science*.**190,** 377-379 (1975).
3. D.A. Bazylinski , R. B. Frankel, Magnetosome formation in prokaryotes. *Nat Rev Microbiol*, **2,** 217-230, (2004).
4. A. Postec, N.Tapia, A. Bernadac, M. Joseph, S.Davidson, L.Fei. Wu, B. Ollivier, N. Pradel, Magnetotactic bacteria in microcosms originating from the French Mediterranean Coast subjected to oil industry activities, *Microb Ecol*. **63**, 1-11, (2012).
5. J. K. Fredrickson, Y. A. Gorby, Environmental processes mediated by iron-reducing bacteria. *Curr. Opin. Biotechnol.* **7**,287-294, (1996).
6. A. Bharde, R. Y. Parikh, M. Baidakova, S. Jouen, B. Hannoyer, T. Enoki, B. L. V. Prasad, Y. S. Shouche, S. Ogale, M. Sastry, Bacteria-Mediated Precursor-Dependent Biosynthesis of Superparamagnetic Iron Oxide and Iron Sulfide Nanoparticles. *Langmuir*. **24**, 5787–5794, (2008).
7. I. Kolinko, A. Lohße , S. Borg, O. Raschdorf, C. Jogler, Q. Tu, M. Pósfai, E. Tompa, J.M. Plitzko, A. Brachmann, G. Wanner, R. Müller, Y. Zhang, D. Schüler, Biosynthesis of magnetic nanostructures in a foreign organism by transfer of bacterial magnetosome gene clusters. *Nat Nanotechnol*. **9,** 193-197, (2014).
8. M. I. Hood, E.P. Skaar, Nutritional immunity: transition metals at the pathogen-host interface. *Nat Rev Microbiol.* **10**, 525-537, (2012).
9. L. Ma, A. Terwilliger, A.W. Maresso, Iron and zinc exploitation during bacterial pathogenesis. *Metallomics,* **7**, 1541-1554, (2015).
10. Z. Xu, P. Wang, H. Wang, Z.H. Yu, H. Y. A. Yeung, T. Hirayama, H. Sun, A.Yan, Zinc excess increases cellular demand for iron and decreases tolerance to copper in *Escherichia coli*. *J. Biol. Chem.* **294,** 16978-16991, (2019).
11. S. C. Andrews, A. K. Robinson, F. Rodríguez-Quiñones, Bacterial iron homeostasis. *FEMS Microbiology Reviews*, **27**, 215–237, (2003).
12. D. A. Capdevila, J. Wang, D.P. Giedroc, Bacterial strategies to maintain zinc metallostasis at the host-pathogen interface. *J Biol Chem.* **291**, 20858-20868, (2016).

13. G.Y. Zhang, Y.Q. Sun, D.Z. Gao, Y.Y. Xu, Quasi-cube $ZnFe_2O_4$ nanocrystals: Hydrothermal synthesis and photocatalytic activity with TiO_2 (Degussa P25) as nanocomposite. *Mater. Res. Bull.* **45**, 755-760, (2010).
14. S.K. Sahoo, G. Hota, Amine-Functionalized GO Decorated with ZnO-$ZnFe_2O_4$ Nanomaterials for Remediation of Cr (VI) from Water. *ACS Appl. Nano Mater.* , **2**, 983–996, (2019).
15. H. Chen, W. Liu, Z.Q, ZnO/$ZnFe_2O_4$ nanocomposite as a broad-spectrum photo-Fenton-like photocatalyst with near-infrared activity. *Catal. Sci. Technol.*, **7**, 2236-2244, (2017).
16. C. Yao, Q. Zeng, G. F. Goya, T. Torres, J. Liu, H. Wu, M. Ge, Y. Zeng, Y. Wang, J. Z. Jiang, $ZnFe_2O_4$ nanocrystals: Synthesis and magnetic Properties. *J. Phys. Chem. C.* **111**, 12274–12278, (2007).
17. T. Hyeon, Chemical synthesis of magnetic nanoparticles. *Chem. Commun.* **8**, 927-934, (2003).
18. M. Mazur, A. Barras, V. Kuncser, A. Galatanu, V. Zaitzev, K.V. Turcheniuk, P. Woisel, J. Lyskawa, W. Laure, A. Siriwardena, R. Boukherroub, S. Szunerits, Iron oxide magnetic nanoparticles with versatile surface functions based on dopamine anchors. *Nanoscale,* 2535 -3084, (2013).
19. J.M. Byrne, V. S. Coker, E. Cespedes, P.L. Wincott, D. J. Vaughan, R.A.D. Pattrick, G. van der Laan, E. Arenholz, F. Tuna, M. Bencsik, J.R. Lloyd, N. D. Telling, Biosynthesis of zinc substituted magnetite nanoparticles with enhanced magnetic properties. *Adv. Funct. Mater.***24**, 2518-2529, (2014).
20. X. Wang, L. Huang, Y. Zhao, Y. Zhang, G. Zhou, Synthesis of mesoporous ZnO nanosheets via facile solvothermal method as the anode materials for Lithium-ion batteries. *NRL*. **11**, 1-6, (2016).
21. B. A. Eijkelkamp, J.R. Morey, M. P. Ween, Cheryl-lynn Y. Ong, A. G. McEwan, J. C. Paton, C. A. McDevitt , Extracellular zinc competitively inhibits manganese uptake and compromises oxidative stress management in *Streptococcus pneumonia. PloS one*, **9**, 1-11, (2014).
22. S. Kaushik, J. Thomas, V.Panwar, H. Ali, V. Chopra, A. Sharma, R. Tomar, D. Ghosh, In situ biosynthesized superparamagnetic iron oxide nanoparticles (SPIONS) induce efficient hyperthermia in cancer cells. A*CS Appl. Bio Mater.* **3**, 779–788, (2020).
23. D. Lucarelli , S. Russo, E. Garman, A. Milano, W.Meyer-Klaucke, E.Pohl, Crystal Structure and Function of the Zinc Uptake Regulator FurB from Mycobacterium tuberculosis. *J. Biol. Chem.* **282**, 9914 –9922, (2007).
24. R. R. Baker, J.G. Mather, J.H. Kennaugh, Magnetic bones in human sinuses. *Nature.* **301**, 78-80, (1983).
25. A. Curcio, A. Van de Walle, A.Serrano, S. Preveral, C. Péchoux, D.Pignol, N.Menguy, C. T. Lefevre, A. Espinosa, C. Wilhelm, Transformation Cycle of Magnetosomes in Human Stem Cells: From Degradation to Biosynthesis of Magnetic Nanoparticles Anew. *ACS Nano.* **14**, 1406–1417, (2020).

26. A. Van de Walle, A. P. Sangnier, A. Abou-Hassan, A. Curcio, M. Hémadi, N. Menguy, Y. Lalatonne, N.Luciani, C.Wilhelm, Biosynthesis of magnetic nanoparticles from nano-degradation products revealed in human stem cells. *PNAS.***116**, 4044-4053, (2019).

Acknowledgements:

We thank Dr. Erik T. J. Nibbering, Max-Born-Institut and Dr. Narayan Pradhan from IACS, Kolkata for critically reviewing the manuscript. The support of Dr. Chayan K. Nandi (IIT, Mandi) and Dr. Suvankar Chakraverty, INST and Dr. Nitin Singhal, NABI is acknowledged. The authors thank Ms. Gurleen Kaur for assistance with graphics. The authors thank Department of Biotechnology (BT/PR22067/NNT/28/1163/2016), Department of Science and Technology (SERB/F/755/2019-2020), India for partially funding the project and INST, Mohali for infrastructure support.

Author contributions:

SK: Investigated, Visualized and compiled the manuscript. JT, RS, HSR and VC: Investigated and visualized the data. VP: Analyzed the data; RK: Supported with microbial cultures; VG provided essential microbial strains, supported the investigations and edited the manuscript. DG: Conceptualized, supervised, secured funding and edited the manuscript. All authors read and approved the final manuscript.

Competing interests: The authors declare no competing financial interest.

All data is available in the main text or the supplementary materials.

Supporting Online Material

Fig. S1-S2, S11-S18

Movies S3 to S10, S19 to S20

Table S1

Materials and Methods: S21.